Implementation and Assessment of Jamming Effectiveness Against an FMCW Tracking Radar Based on a Novel Criterion

MOHAMMAD REZA ZAKERHAGHIGHI
MOHSEN MIVEHCHY
MOHAMMAD FARZAN SABAHI, Member, IEEE
University of Isfahan, Isfahan, Iran

The effect of jammer on radar or jamming performance has been and is being assessed on the basis of range reduction where consistency in tracking target ability is more important than range reduction in a tracking radar. A new criterion known as relative radar functionality destruction time is defined and introduced as the relative of functionality destruction time of radar to one period of jammer, where jammer signal and target echo power are of concern. The effective parameters in relative time of the receiver functioning destruction are assessed. Next, this criterion is applied in the assessment of simple conical scan radar receiver against a conventional jamming (sweep noise jamming). This criterion is modeled and simulated on a search radar in the jamming environment where the minimum required standard deviation of noise for destroying the radar function yields. By implementing the structure of a frequency modulated continuous wave tracking radar structure, a simple target based on digital radio frequency memory method and one type of jamming against this radar in a simultaneous manner, the functionality destruction is extracted for different radar parameters. This new criterion on outperforms its counterparts.

Manuscript received August 1, 2019; revised February 14, 2020 and May 27, 2020; released for publication May 27, 2020. Date of publication June 19, 2020; date of current version December 4, 2020.

DOI. No. 10.1109/TAES.2020.3000001

Refereeing of this contribution was handled by K. S. Kulpa.

Authors' address: The authors are with the Department of Electrical Engineering, Faculty of Engineering, University of Isfahan, Isfahan 8174673441, Iran E-mail: (m.zakerhaghighi@eng.ui.ac.ir, mivehchy@eng.ui.ac.ir, sabahi@eng.ui.ac.ir). *(Corresponding author: Mohsen Mivehchy.)*

I. INTRODUCTION

With the advances made in radar systems during the WWII, electronic countermeasure systems and electronic counter-countermeasure systems appeared. It is necessary to analyze the effects of jamming on different types of radars to choose the appropriate method for interfering or confronting with interference in such systems [1], [2]. Consequently, this issue in radar systems and different types of jamming, necessitates assessments to be run on the effects of jamming which is a complicated matter, usually with uncertain answers [3]. In some of the available methods, the jamming effect is analyzed based on the reduction of radar range or the error ratio of range extraction [4], velocity, and angular error in target tracking radar (TTR) systems [5], [6]. The target tracking error is related to the jamming power to signal power ratio, j/s, and a criterion is introduced in this regards named coefficient of suppression of the target tracking error power [7]. The signal power to the jamming power ratio, S/J, receiver characteristics, signal processing methods, and the type of modulation are generally considered for the abovementioned ratios [8]–[10]. In the presence of a jammer, the signal power to the total power of noise and jammer ratio, S/N+J, decreases leading to a maximum range reduction. To assess the effectiveness of the jammer, the maximum range in the presence of jammer is compared with the maximum range in the absence of jammer [11], [12]. When features like target tracking and locking capabilities are of concern, the existing criteria are not so appropriate; because in most operational environments, the time duration of radar's basic functions destruction (e.g., tracking ability) is more important than the ratio of range reduction and the speed or angle error ratio. Therefore, in this article, the criterion of the relative receiver functionality destruction time, presented in [13], optimized based on the effect of a conventional jamming on a simple conical scan tracking radar with fixed operating frequency is assessed.

The objective here is to assess the impact of conventional jamming on tracking radar function, based on a theoretical model and experimental results.

II. MODELING OF THE DIRECT NOISE JAMMING

The noise jamming, obtained through the direct amplification of microwave band noise can be expressed through

$$u_j(t) = u_n(t).\cos(2\pi f_j t + \phi(t)) \tag{1}$$

where $u_n(t)$ is the instantaneous amplitude of the noise, $u_j(t)$ has the Gaussian distribution, $\phi(t)$ has the uniform distribution in $[0-2\pi]$ interval and are independent, f_j is the carrier frequency with a fixed value. The noise power is limited and its power spectrum expressed [14] by

$$G_j(f) = \begin{cases} \frac{\sigma^2}{\Delta f_j} & |f - f_j| \le \frac{\Delta f_j}{2} \\ 0 & \text{others} \end{cases} \tag{2}$$

where σ^2 is the average noise power, Δf_j is the jamming bandwidth, and f_j is the jamming central frequency.

If the receiver intermediate frequency (IF) filter is of a rectangular characteristic, after passing the noise through

the receiver, the noise at the output of the IF amplifier is a bandlimited Gaussian noise and its power spectrum is expressed as shown in

$$G_i(f) = |H_i(f)|^2.G_j(f - f_i) = \begin{cases} \frac{\sigma^2}{\Delta f_i} & |f - f_i| \le \frac{\Delta f_i}{2} \\ 0 & \text{others} \end{cases} \tag{3}$$

where f_i is the center frequency of the receiver, $H_i(f)$ is the equivalent frequency response in IF bandwidth, and Δf_i is the receiver IF bandwidth.

The autocorrelation function of the noise in the IF band is expressed through (4) by using the Fourier transform relation between the autocorrelation function and the power spectrum density function

$$R_i(\tau) = \int_0^\infty G_i(f)\cos(2\pi f\tau)df. \tag{4}$$

After linear detection, the Gaussian white noise distribution is transformed into Rayleigh distribution [14], expressed through

$$P_i(u_v) = \frac{u_v}{\sigma_v^2} e^{\frac{u_v^2}{2\sigma_v^2}}, \qquad u_v > 0 \tag{5}$$

where $\sigma_v^2 = k\sigma^2$ and k is the linear detector gain factor. In practice, RF noise signals and radar signals are collected by the radar receiver, where the final output signal is the sum of the both signals.

The echo signal from the target is a single-frequency signal, expressed in

$$s(t) = u_s.\cos(2\pi f_0 t) \tag{6}$$

where u_s and f_0 are amplitude and frequency, respectively.

The output sum signal and the final output signal in the IF band are expressed through

$$u_j(t) + s(t) = \begin{cases} u_n(t).\cos(2\pi f_j t + \phi(t)) + u_s.\cos(2\pi f_0 t) \\ \text{(in RF band)} \\ u_i(t).\cos(2\pi f_i t + \phi(t)) \\ \text{(in IF band)} \end{cases} \tag{7}$$

where $u_i(t)$ is the amplitude of the ultimate output sum signal with Rician distribution. In range gate pull-off (RGPO), deception jamming technique, the strong radio frequency (RF) pulse which is similar to the target echo, is used to capture the range gate in the receiver's processor and pull it off away. For RGPO deception jamming, the echo signal and the jammer signal are modeled [14] in

$$s_s(t) = a_s \exp\left[j(2\pi f_c + 2\pi f_d)\left(t - \frac{2R(t)}{c}\right)\right] \tag{8}$$

$$s_j(t) = a_j \exp\left[j(2\pi f_c + 2\pi f_d)\left(t - \frac{2R(t)}{c} - \Delta t_j(t)\right)\right] \tag{9}$$

where a_s and a_j are the actual target signal amplitude and the interference signal amplitude, respectively, in a sense that $a_j > a_s$. The parameter f_c is the carrier frequency of the radar, f_d is the doppler frequency, $R(t)$ is the target range, c is the light speed, and Δt_j is the jammer signal delay. Assuming the different states in the RGPO deception jamming and the target is moving at a constant velocity of v_1, the target delay time function $\Delta t_j(t)$ is expressed through (10) and (11) for capture and RGPO time intervals

$$\Delta t_j(t) = \frac{r + v_1.t}{c} \quad 0 \le t < t_1 \quad \text{(capture phase)} \tag{10}$$

$$\Delta t_j(t) = \frac{r + v_1.t + v_2.(t - t_1)}{c} \quad t_1 \le t < t_2 \text{ (pull of phase)} \tag{11}$$

where r is the target range, v_1 is the target speed, v_2 is the jammer velocity, $0 \le t < t_1$ is the capture time interval and $t_1 \le t < t_2$ is the rage gate pull off time interval. Modeling of other types of noise jamming are also presented in [1] and [3].

III. NOISE JAMMING EFFECTS ON RADAR PERFORMANCE ASSESSMENT

The jamming effect is assessed through the $\frac{j}{s}$ ratio [8], expressed in

$$\frac{j}{s} = \left(\frac{4\pi}{\sigma(\text{SPG})}\right)\left(\frac{P_j}{P_R}\right)\left(\frac{G_j G_{\text{Rj}}}{G_{\text{RT}}^2}\right)\left(\frac{B_j}{B_R}\right)\left(\frac{R_T^4}{R_j^2}\right) \tag{12}$$

where P_R is transmitter power, G_{RT} is the radar antenna gain in target direction, σ is the radar cross section, P_j is the jammer power, G_j is the jammer antenna gain in radar direction, G_{Rj} is the radar antenna gain in jammer direction, SPG is the radar signal processing gain, R_j is the range to jammer, R_T is the range to target, B_R is the radar receiver bandwidth, and B_j is the jammer noise bandwidth.

The range obtained from (12) is named R_{TS}, assuming $j/s = 1$ or 0 dB

$$R_{Ts}^4 = \left(\frac{\sigma(\text{SPG})R_J^2}{4\pi}\right)\left(\frac{P_R}{P_j}\right)\left(\frac{G_{\text{RT}}^2}{G_J G_{\text{Rj}}}\right)\left(\frac{B_R}{B_j}\right) \tag{13}$$

where $R_T = R_{Ts}$.

The radar performance in the presence of jamming is assessed by [7]. It should be noted that in a TTR when features like target tracking persistence or track quality are of concern, the previous assessment is not enough for destruction time of the radar function, therefore the need for a new criterion becomes essential, where the proper functioning time absent in the previous assessments is of concern to make the mission of the radar system more consistent.

IV. RELATIVE RECEIVER FUNCTIONALITY DESTRUCTION TIME CRITERION

A criterion is proposed by [13] for assessing sweep noise jamming effect on some types of radar based on the relative radar functionality destruction time. In this criterion, both the jamming power and signal power are considered at the input of the radar receiver. The parameters $X_s(t, f)$ and $X_j(t, f)$ are considered as component of the received signals from the target and the jammer at the receiver input, depending on the radar type, the transmitted signal modulation,

the target specification, and the method of jamming are functions of time and frequency.

When the jammer's center frequency is far from the radar's center frequency, there is no overlap between receiver and jammer bands, the jammer energy is not injected into the radar receiver band, thus, nonoccurrence of functionality degradation; consequently, to have functionality destruction of the receiver in determining the parameter α (the α parameter may be the range, speed, angular error, or ability to keep lock). The jammer spectrum should be overlapped with the receiver's effective bandwidth in determining the desired parameter ($B_{R,\alpha}$).

For assessing the jamming effect, the jammer influence coefficient ($\mu^j_{R,\alpha}$) which is defined through the two following ratios is commonly used:

1) the receiver functionality destruction time in determining the parameter α, $T_{D,\alpha}$, to the total time of a jamming sweep period (T_S) ratio;
2) the average power of received jamming signal ($\overline{P^j_R}$) to the average power of the received signal from the target ($\overline{P^s_R}$) ratio at the input of the receiver during the jamming sweep period.

The jamming effect coefficient in determining the parameter α is expressed in

$$\mu^j_{R,\alpha} = \frac{\frac{T_{D,\alpha}}{T_S}}{\frac{\overline{P^j_R}}{\overline{P^s_R}}} = \frac{T_{D,\alpha}}{T_S}.\frac{\overline{P^s_R}}{\overline{P^j_R}} \tag{14}$$

where

$$\overline{P^j_R} = \frac{1}{T_S}\int_{T_S}\int_{B_j} X_j(t,f)dfdt \tag{15}$$

$$\overline{P^s_R} = \frac{1}{T_S}\int_{T_S}\int_{B_{R,\alpha}} X_s(t,f)dfdt. \tag{16}$$

B_j and $B_{R,\alpha}$ are the jamming spectral bandwidth and receiver effective bandwidth in determining α, respectively. Moreover, the receiver proper functioning time (in determining the parameter α, $T_{p,\alpha}$, to the total jamming sweep period ratio is obtained through

$$\frac{T_{p,\alpha}}{T_S} = 1 - \frac{T_{D,\alpha}}{T_S}. \tag{17}$$

Because the overlapping time duration of the jammer spectrum with receiver effective bandwidth in determining the parameter α is equal to $T_{D,\alpha}$, but the radar system processor during the overlapping time, runs subject to the main capabilities in target tracking, which is the ability of target angular tracking or detecting the existence of the target, which are not generally disturbed after crossing the jammer from the receiver band, where the radar immediately proceeds to previous target tracking situation and extracts the target information. On the contrary, provided that the radar system tolerance duration at the destruction time of α parameter ($T_{K,D,\alpha}$) is less than ($T_{D,\alpha}$), the overall performance of the radar system is disrupted, then no more target lock, necessitating a recovery time of T_{Renew} to restore

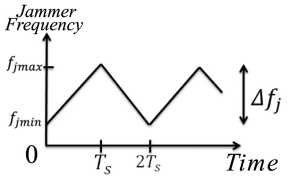

Fig. 1. Central frequency of the sweep jammer versus time.

the target. If the α is considered as range or speed of the target, then at the end of the jammer spectrum crossing with receiver bandwidth and after a short overhead time ($T_{\text{OH},\alpha}$), the range and speed extraction is resumed. $T_{\text{OH},\alpha}$ is the necessary time for retrying to find target and extraction of α parameter after every target missing. Accordingly, the total destruction time for this parameter is equal to $T_{D,\alpha} + T_{\text{OH},\alpha}$. Moreover, if the parameter α to be the ability of track and keeping the lock on target and $T_{D,\alpha} > T_{K,D,\alpha}$, the lock on the target breaks, and target tracking resumes after recovery time T_{Renew}, which may be long. Therefore, in this situation, the actual destruction time of the α parameter is completely different from the previous values in determining the range and speed, and is equal to $T_{D,\alpha} + T_{\text{Renew}}$, which indicates a nonlinear behavior, and a significant increase in the jamming effect coefficient on the receiver ($\mu^j_{R,\alpha}$).

V. Relative Destruction Time Criterion in Assessing the Effect of Sweep Noise Jamming Application

Here, the jammer signal with B_j spectrum bandwidth sweeps the frequency bandwidth Δf_j at a frequency sweep rate which is known as V_j (Hz/s) in a linear manner over time T_S. The central frequency of the jamming spectrum is expressed by f_j and its variation versus time is illustrated in Fig. 1, where the jamming sweep width and V_j are $\Delta f_j = f_{j\max} - f_{j\min}$ and $V_j = \frac{\Delta f_j}{T_S}$, respectively.

In this assessment a simple model is considered where the radar receiver has a fixed bandwidth, and it is assumed that this bandwidth is located in the jammer sweeping bandwidth; the power spectrum of the jamming signals and the received signal from the target at the receiver input are shown in Fig. 2(a) and (b), respectively.

When jammer, with the aim of interfering with the radar, moves in Δf_j bandwidth, its crosses with the receiver bandwidth over the time T_I. The overlap of the jamming and receiver bands ($B_I(t)$) versus time is shown in Fig. 2(c) and the relation between the parameters are expressed in

$$B_{I\max} = \min(B_{R,\alpha}, B_j) \tag{18}$$

$$T_{J\max} = \frac{|B_{R,\alpha} - B_j|}{\Delta f_j} T_S \tag{19}$$

$$t'_1 = \frac{B_{I\max}}{\Delta f_j} T_S \tag{20}$$

$$T_I = 2t'_1 + T_{J\max} = \frac{2B_{I\max} + |B_{R,\alpha} - B_I|}{\Delta f_j} T_S,\ T_I \le T_S. \tag{21}$$

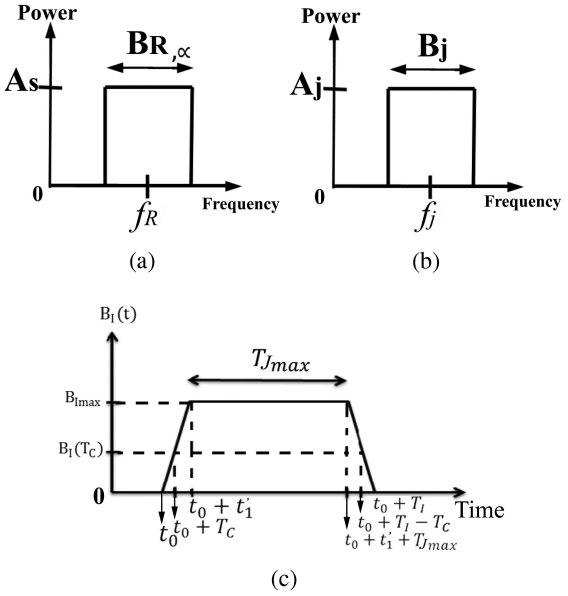

Fig. 2. (a) Jammer power spectrum. (b) Target signal spectrum at the receiver input. (c) Jamming and receiver overlap versus time [13].

A. Relative Functionality Destruction Time

To determine the parameter α in an accurate manner, the signal power to the part of the jammer power (located into the receiver bandwidth) ratio must not be reduced to a specific value. This ratio, PR^{sj}, is expressed in

$$\overline{PR^{\mathrm{sj}}} = \frac{P^s(t)}{P^j(t)} = \frac{\int_{B_{R,\alpha}} X_s(t,f)df}{\int_{B_{R,\alpha}} X_j(t,f)df}. \tag{22}$$

By moving the jammer spectrum toward the receiver band, a simultaneous gradual increase in the overlap bandwidth ($B_I(t)$) and a decrease in the receiver performance in determining the parameter α take place. The minimum value of PR^{sj}, where the receiver performance begins to degrade isobtained by K_α^j in

$$PR^{\mathrm{sj}} = \frac{A_s B_{R,\alpha}}{A_j B_I(T_C)} \le K_\alpha^j. \tag{23}$$

Where, A_s and A_j are the signal and jammer power, respectively. $B_I(T_C)$ is the overlap threshold value of the bands, where all lead to the receiver functionality destruction time $t = T_C$, and is defined in:

$$B_I(T_C) = \frac{A_s B_{R,\alpha}}{A_j K_\alpha^j} \tag{24}$$

where

$$T_C = \frac{A_s B_{R,\alpha}}{A_j K_\alpha^j \Delta f_j} T_S, \qquad T_C \le T_S. \tag{25}$$

The duration of the receiver performance destruction ($T_{D,\alpha}$) is expressed in

$$T_{D,\alpha} = T_S \left(\frac{2B_{I\max}}{\Delta f_j} + \frac{|B_{R,\alpha} - B_j|}{\Delta f_j} - \frac{2B_{R,\alpha}A_s}{\Delta f_j K_\alpha^j} \right) \tag{26}$$

where $B_{I\max}$ is the largest value of bands overlapping. For different ratios of $\frac{B_{R,\alpha}}{B_j}$ $\left(\frac{B_{R,\alpha}}{B_j} \le 1 \text{ and } \frac{B_{R,\alpha}}{B_j} > 1\right)$, in the first case, the $B_{R,\alpha}$ is smaller than B_j and $B_I\max = B_{R,\alpha}$ and $T_{D,\alpha}$ is expressed in

$$T_{D,\alpha} = \frac{1}{N}\left[\left(\frac{B_{R,\alpha}}{B_j}\right) + 1 - \left(\frac{B_{R,\alpha}}{B_j}\right)\frac{2A_s}{A_j K_\alpha^j} \right].T_S \tag{27}$$

where $N = \frac{\Delta f_j}{B_j}$, in the second case, $B_{R,\alpha}$ is greater than B_j, $B_{I\max} = B_j$, and the $T_{D,\alpha}$ is similar to the (27).

According to the above-mentioned data, it can be easily inferred that, both the cases lead to the same result. In addition, the relative receiver destruction functioning time has a nonlinear relation with the receiver and jammer parameters.

Given the initial assumption for the jammer and the received signal spectrums, as observed in Fig. 2(a) and (b), the average value of the jammer and the target echo signal powers at the receiver input, according to (15) and (16), can be obtained through

$$\overline{P_R^j} = B_J.A_j \tag{28}$$

$$\overline{P_R^s} = B_{R,\alpha}.A_s. \tag{29}$$

By applying (15), (18), (27), and (28), the jamming effect coefficient is expressed in

$$\mu_{R,\alpha}^j = \frac{1}{N}\left[1 + \left(\frac{B_{R,\alpha}}{B_j}\right)\left(1 - \left(\frac{A_s}{A_j}\right)\left(\frac{2}{K_\alpha^j}\right)\right)\right]\left(\frac{A_s.B_R,\alpha}{A_j.B_j}\right). \tag{30}$$

B. Simulation of Sweep Noise Jammer Versus Receiver's Bandwidth

The objective of the assessment is to choose the appropriate relative bandwidth for the radar receiver to improve the receiver performance versus the sweep noise jammer for different j/s. The MATLAB software is used to derive many curves for the relative time of receiver proper functionality and the destruction coefficient for various values of $\frac{B_j}{B_{R,\alpha}}$, $\frac{A_j}{A_s}$, and K_α^j.

The receiver proper functionality time (T_P) to a period of the jammer sweep (T_S) ratio, $\frac{Tp,\alpha}{T_S}$ versus Aj/As is shown in Fig. 3 for different ratios of $\frac{B_j}{B_{R,\alpha}} = 0.1, 0.5, 1, 5$. Two issues can be concluded from these curves as follows.

By increasing j/s in the radar receiver, the proper functionality time is reduced, and for small values of $\frac{B_j}{B_{R,\alpha}}$, a decrease in the receiver proper functionality begins at greater values of $\frac{A_j}{A_s}$ and thereafter, with a slight increase in $\frac{A_j}{A_s}$, the proper functionality time decreases significantly. However, for the higher values of $\frac{B_j}{B_{R,\alpha}}$, the reduction of the receiver proper functionality time begins at lower values of $\frac{A_j}{A_s}$; note that after a specific $\frac{A_j}{A_s}$ ratio, an excessive increasing in the $\frac{A_j}{A_s}$ has a significant effect on the proper functionality of the receiver.

A tradeoff can be made between the two previous states to introduce a proper state, the receiver function destruction

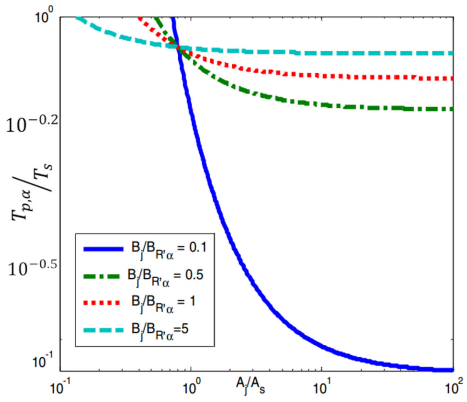

Fig. 3. $\frac{T_{P,\alpha}}{T_S}$ in the case of sweep noise jamming versus $\frac{A_j}{A_s}$ for values $\frac{B_j}{B_{j,\alpha}} = 0.1, 0.5, 1, 5$.

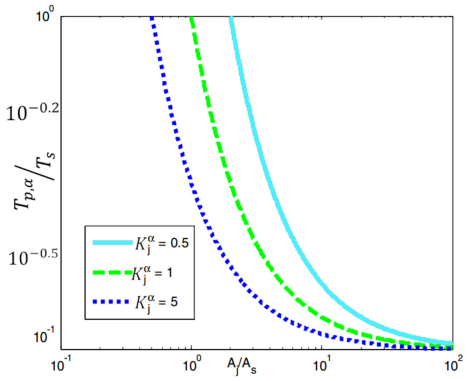

Fig. 4. $\frac{T_{P,\alpha}}{T_S}$ versus $\frac{A_j}{A_s}$ for values $K_\alpha^J = 0.5, 1, 2$.

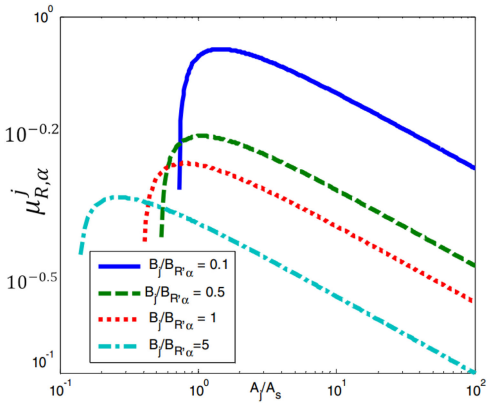

Fig. 5. $\mu_{R,\alpha}^j$ versus $\frac{A_j}{A_s}$ for values $\frac{B_j}{B_{R,\alpha}} = 0.1, 0.5, 1.5$.

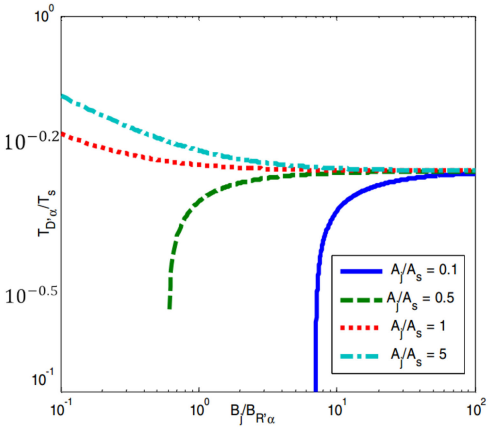

Fig. 6. $\frac{T_{D,\alpha}}{T_S}$ versus $\frac{B_j}{B_{R,\alpha}}$ for values $\frac{A_j}{A_s} = 0.1, 0.5, 1.5$.

begins at higher values of $\frac{A_j}{A_s}$, and the reduction rate of the receiver proper functionality time with a slight increase in $\frac{A_j}{A_s}$ (e.g., the relative bandwidth of $\frac{B_j}{B_{R,\alpha}} = 1$ can be chosen as a compromise between two states.)

From Fig. 3 and (27), it is deduced that despite the overlapping of the bands, the receiver functionality is not degraded ($T_{D,\alpha} = 0$), and this state can be accomplished through

$$\frac{B_{R,\alpha}}{B_j} = \frac{K_\alpha^j\left(\frac{A_j}{A_s}\right)}{2 - K_\alpha^j\left(\frac{A_j}{A_s}\right)} \tag{31}$$

$$\frac{A_j}{A_s} = \frac{K_\alpha^j}{2}\left(\frac{1}{\frac{B_{R,\alpha}}{B_j}} + 1\right). \tag{32}$$

With some basic information of jammer and radar characteristics (B_j, A_j), the effective receiver bandwidth and minimum radar transmitter power can be determined through (31) and (32) to prevent degradation in the receiver performance.

$\frac{T_{p,\alpha}}{T_S}$ for values of $K_\alpha^j = 0.5, 1, 2$ as a function of $\frac{A_j}{A_s}$, are shown in Fig. 4, where there is a decrease in K_α^j, the receiver function destruction that begins at higher values of $\frac{A_j}{A_s}$.

The jamming destruction coefficient $(\mu_{R,\alpha}^j)$ variations as a function of $\frac{A_j}{A_s}$ for some values of jammer-relative bandwidth, $\frac{B_j}{B_{R,\alpha}}$, is depicted in Fig. 5, where, as observed in the case of high $\frac{B_j}{B_{R,\alpha}}$, a significant loss in receiver functionality begins at a smaller value of $\frac{A_j}{A_s}$ and with an increase in $\frac{A_j}{A_s}$, the $\mu_{R,\alpha}^j$ decreases. However, when the relative bandwidth of the jammer is low, the significant loss in the receiver begins at higher values of $\frac{A_j}{A_s}$; after which, with increasing in $\frac{A_j}{A_s}$, the jamming destruction coefficient decreases. In both cases, if the jammer power in the receiver band exceeds the threshold level, the $\mu_{R,\alpha}^j$ increases for high relative receiver bandwidth as well, that is, the influence of jammer and the relative functionality destruction time of α increases.

The $\frac{T_{D,\alpha}}{T_S}$ (relative destruction time) variations for the values of $\frac{A_j}{A_s} = 0.1, 0.5, 1.5$ as a function of $\frac{B_j}{B_{R,\alpha}}$, is shown in Fig. 6, where increasing in $\frac{B_j}{B_{R,\alpha}}$, the relative destruction time remains constant for all different values of the $\frac{A_j}{A_s}$.

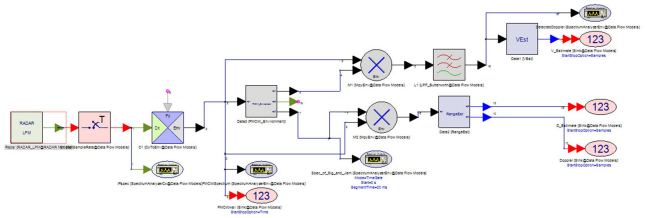

Fig. 7. Simulation of FMCW-search radar in presence of barrage jamming.

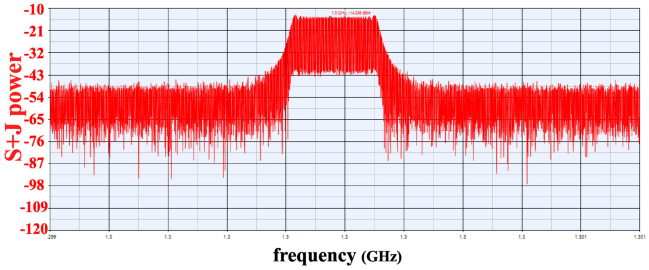

Fig. 8. Receiver output spectrum, in the presence of Target and barrage jamming with STD = 0.5.

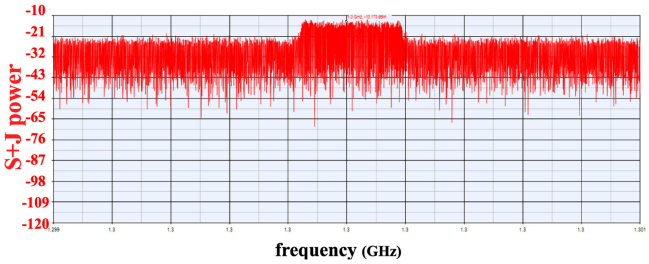

Fig. 9. Receiver output spectrum, in the presence of target and barrage jamming with STD = 10.

VI. SIMULATION AND IMPLEMENTATION OF RADAR SYSTEM IN JAMMING ENVIRONMENT

In this section, in subsection A, the simulation and its results of a frequency modulated continuous wave (FMCW)-search radar performance in jamming environment, and in subsection B, hardware implementation of the fixed bandwidth radar receiver and transmitter is presented.

A. FMCW-Search Radar Performance in Jamming Environment Simulation

As for the simulation scene, here, it is assumed that the echo signal bandwidth, BW = 200 kHz, $T_d = 200\ \mu$s, range = 30 km, $f_c = 10$ GHz, $f_d = 15$ kHz, $\Delta f_{\max} = 40$ kHz. The transmitter and receiver for linear frequency modulated continuous wave (LFMCW) radar in the presence of jammer are modeled and simulated through Keysight SystemVue software. The simulation of the radar structure is shown in Fig. 7 and their responses versus for several standard deviations (STD) of power jamming are shown in Figs. 8–10.

The results obtained for different STD of barrage jamming that is injected to radar receiver are tabulated in Table I.

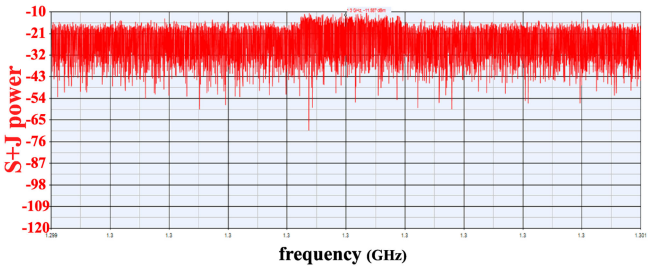

Fig. 10. Receiver output spectrum, in the presence of target and barrage jamming with STD = 20.

TABLE I
Results Obtained for Several STD of Barrage Jamming

STD	Velocity (km/hr)	Range (km)	Destruction
0.1	810	29.48	No
0.2	810	29.48	No
0.5	810	29.48	No
1	810	29.48	No
2	810	29.48	No
5	810	5506.641	Yes
10	810	5506.641	Yes

Although, these results are related to FMCW-search radar, which only detects target, range, and velocity, it provides a promising aspect for the minimum jammer power in destroying the radar function.

B. Hardware Implementation of the Fixed Bandwidth Radar Receiver and Transmitter

The design and implementation of this hardware consist of: 1) the transmitter (low powered); 2) receiver part of the fixed frequency tracking radar; and (3) the sweep noise jammer simulator circuit. The main features of the radar system are as follows.

1) The radar is FMCW type with fixed frequency transmitter (f_c), and the positioning system is conical scan type with scan frequency of $f_s \simeq 40$ Hz. The transmitted signal has sinusoidal FM modulation with modulating frequency of $f_m = 30$ Hz for ranging. Also, the transmitter frequency is constant, at approximately 10 GHz, and the maximum transmitter frequency deviation is $\Delta f_T = 20$ kHz.
2) In order to eliminate the low-frequency component due to transmitter signal phase noise and the effects of the conical sweep, the frequency components in the band 0–2 kHz are removed from the received signal. The total receiver bandwidth is about 100 kHz (or equivalent to target velocity of 4.5 Mach).

During the radar antenna movement, the target appears at the 3 dB antenna beamwidth over the time ($T_{\text{DWELL}} \simeq 100$ ms), the same time is required to save a packet of input data in the time domain for fast Fourier transform (FFT) unit, and the following processes (T_{storage}).

The effective receiver bandwidth for detection of the target is $B_{R,D} \simeq 1$ kHz and the threshold level for target detection is $S/N \geq 6$ dB for under test radar. The maximum tolerance time for the target loss is $T_{K,D,\alpha} \simeq 2$s; provided

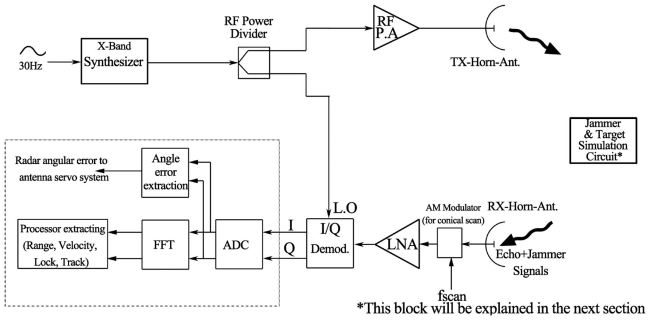

Fig. 11. Simplified block diagram of the X-band radar with conical scan.

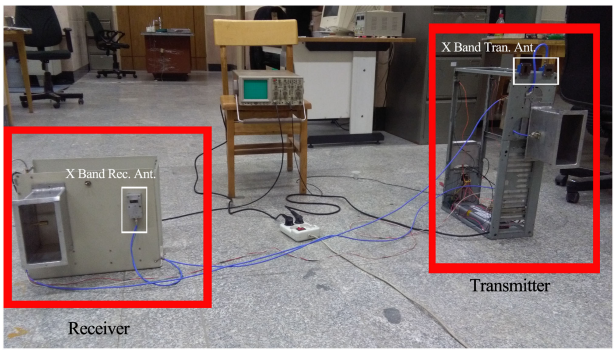

Fig. 12. Setup of X-band radar transmitter and receiver simulator.

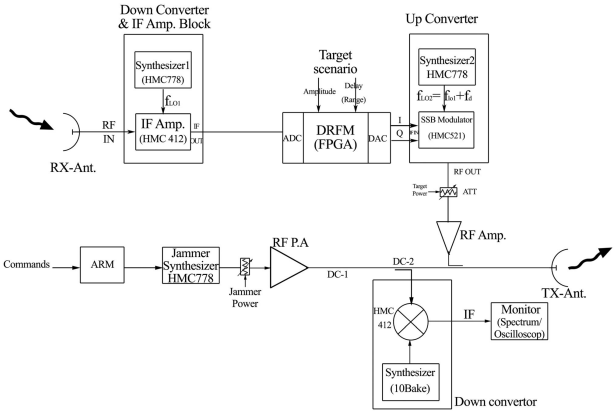

Fig. 13. Jammer and target simulator circuit blocks.

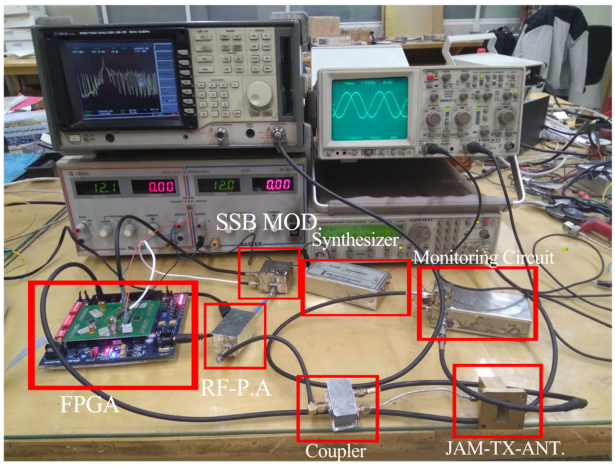

Fig. 14. Setup of the implemented jammer generator and the target.

that during this time, the target does not confirm again the lock on the target breaks and the antenna movement begins, where target new-search resumes. By assuming that the target is still in its previous location and remains at the 3-dB antenna beamwidth, the target recovery time (T_{Renew}) is about 200 ms.

The effective receiver bandwidth for extracting the target radial velocity v_r, $B_{R,v}$, and the minimum signal to noise ratio, S/N, for determining the speed with the appropriate accuracy are expressed as follows:

$$B_{R,v} \simeq 150 \text{ Hz}, \qquad S/N \geq 6 \text{ dB}. \tag{33}$$

The effective receiver bandwidth in extraction of the target range ($B_{R,r}$) and the minimum S/N for determining the target range in a sense that the maximum error remains small are expressed as follows:

$$B_{R,r} \simeq 150 \text{ Hz}, \qquad S/N \geq 12 \text{ dB}. \tag{34}$$

The effective bandwidth for determining the angular tracking error for azimuth and elevation is several times greater than f_s and is about 700 Hz

$$B_{R,\phi} = B_{R,\theta} \simeq 700 \text{ Hz}. \tag{35}$$

Because of the large time constant of the antenna positioning system, the extracted values for the angular error integrated and the effective bandwidth is smaller than 700 Hz. The minimum S/N in angular tracking error in the azimuth and elevation directions is expressed as

$$S/N \geq 6 \text{ dB}. \tag{36}$$

The sinusoidal FM modulation for ranging is run by applying an X-band synthesizer with a 30-Hz frequency signal, the output signal of which enters the RF power divider as shown in Fig. 11. One of the power divider outputs is amplified by a power amplifier (MKU PA 2M-60 W from Kuhne Electronic), and the X-band amplified signal is radiated by transmitting, TX, horn antenna. The echo signals together with the jammer are received by the receiver horn antenna and an AM modulator simulates the action of the conical scan. At this point, the signal is amplified by the LNA circuit and enters in the orthogonal (I/Q) demodulator which applied a HMC521 chip and its baseband outputs signal (I and Q) enters in the analog to digital converter (ADC). The local oscillator signal for down conversion is a sample of transmitted signal transmitted from RF power divider. The digitized I/Q output signals enter the FFT unit and angle error extraction circuits. The processor board is a fast digital signal processing, card (DSK TMS6416 from Texas Instrument) and the ADC board is THS1206EVM (Texas Instrument). The output signal of the FFT unit goes to the processor for additional processing.

The implemented receiver and transmitter system are shown in Fig. 12. Where the blocks for both the X and L bands are evident, only the X-band section of the overall system is of concern in this article.

TABLE II
Relative Destruction Time Results With Different Values of $\frac{A_j}{A_s}$ and $\frac{B_j}{B_{R,\alpha}}$ for $\alpha =$ Target (Left Column) and $\alpha =$ Angle (Right Column), $T_S = 2.5$ s, $\Delta f_j = 250$ MHz, $N = 25$, and $S/J = 6$ dB

α=Target				α=Angle			
$\frac{A_j}{A_s}(dB)$	$\frac{B_j}{B_{R,Detect}}$	$T_{D,Detect}(ms)$	$\frac{T_{D,Detect}}{T_s}(\%)$	$\frac{A_j}{A_s}(dB)$	$\frac{B_j}{B_{R,Angle}}$	$T_{D,Angle}(ms)$	$\frac{T_{D,Angle}}{T_s}(\%)$
-10	$\frac{10MHz}{1kHz}$	0	0	-10	$\frac{10MHz}{700Hz}$	0	0
-10dB	$\frac{1MHz}{1kHz}$	0	0	-10	$\frac{1MHz}{700Hz}$	0	0
-10	$\frac{100kHz}{1kHz}$	0	0	-10	$\frac{100kHz}{700Hz}$	0	0
-10	$\frac{10kHz}{1kHz}$	0	0	-10	$\frac{10kHz}{700Hz}$	0	0
-10	$\frac{1kHz}{1kHz}$	0	0	-10	$\frac{1kHz}{700Hz}$	0	0
0	$\frac{10MHz}{1kHz}$	100.0050	4.0002	0	$\frac{10MHz}{700Hz}$	100.0035	4.00014
0	$\frac{1MHz}{1kHz}$	100.0498	4.0019	0	$\frac{1MHz}{700Hz}$	100.0348	4.001392
0	$\frac{100kHz}{1kHz}$	100.4976	4.0199	0	$\frac{100kHz}{700Hz}$	100.3483	4.013932
0	$\frac{10kHz}{1kHz}$	104.9761	4.1990	0	$\frac{10kHz}{700Hz}$	103.4833	4.139332
0	$\frac{1kHz}{1kHz}$	149.7614	5.99904	0	$\frac{1kHz}{700Hz}$	134.8330	5.39332
10	$\frac{10MHz}{1kHz}$	100.0095	4.00038	10	$\frac{10MHz}{700Hz}$	100.0066	4.000264
10	$\frac{1MHz}{1kHz}$	100.095	4.0038	10	$\frac{1MHz}{700Hz}$	100.0665	4.00266
10	$\frac{100kHz}{1kHz}$	100.9498	4.037992	10	$\frac{100kHz}{700Hz}$	100.6648	4.026592
10	$\frac{10kHz}{1kHz}$	109.4976	4.379904	10	$\frac{10kHz}{700Hz}$	106.6483	4.265932
10	$\frac{1kHz}{1kHz}$	194.9761	7.799044	10	$\frac{1kHz}{700Hz}$	166.4833	6.659332
20	$\frac{10MHz}{1kHz}$	100.0099	4.000396	20	$\frac{10MHz}{700Hz}$	100.0070	4.00028
20	$\frac{1MHz}{1kHz}$	100.0995	4.00398	20	$\frac{1MHz}{700Hz}$	100.0696	4.002784
20	$\frac{100kHz}{1kHz}$	100.9950	4.0398	20	$\frac{100kHz}{700Hz}$	100.6965	4.02786
20	$\frac{10kHz}{1kHz}$	109.9498	4.397992	20	$\frac{10kHz}{700Hz}$	106.9648	4.278592
20	$\frac{1kHz}{1kHz}$	199.4976	7.979904	20	$\frac{1kHz}{700Hz}$	169.6483	6.785932
30	$\frac{10MHz}{1kHz}$	100.0100	4.0004	30	$\frac{10MHz}{700Hz}$	100.0070	4.00028
30	$\frac{1MHz}{1kHz}$	100.0999	4.003996	30	$\frac{1MHz}{700Hz}$	100.0700	4.0028
30	$\frac{100kHz}{1kHz}$	100.9995	4.03998	30	$\frac{100kHz}{700Hz}$	100.6996	4.027984
30	$\frac{10kHz}{1kHz}$	109.9950	4.3998	30	$\frac{10kHz}{700Hz}$	106.9965	4.27986
30	$\frac{1kHz}{1kHz}$	199.9498	7.997992	30	$\frac{1kHz}{700Hz}$	169.9648	6.798592
40	$\frac{10MHz}{1kHz}$	100.0100	4.0004	40	$\frac{10MHz}{700Hz}$	100.0070	4.00028
40	$\frac{1MHz}{1kHz}$	100.1000	4.004	40	$\frac{1MHz}{700Hz}$	100.0700	4.0028
40	$\frac{100kHz}{1kHz}$	100.9999	4.039996	40	$\frac{100kHz}{700Hz}$	100.7000	4.028
40	$\frac{10kHz}{1kHz}$	109.9995	4.39998	40	$\frac{10kHz}{700Hz}$	106.9996	4.279984
40	$\frac{1kHz}{1kHz}$	199.9950	7.9998	40	$\frac{1kHz}{700Hz}$	169.9965	6.79986

1) *Jammer and Target Hardware Implementation:* By assuming the jammer is self-protected (located on the target) with sweep noise type and its bandwidth is B_j, which linearly sweeps frequency bands of $f_{j,\min} \sim f_{j,\max}$ during $T_S = 2.5$ s, where the jammer transmitter has a constant power. Hence, with an increase in the B_j, the A_j/A_s reduces. The bandwidth B_j and the upper and lower ranges of the frequency sweep are selectable by the advanced RISC machine microcontroller board. The digital radio frequency memory (DRFM) technique is applied for target signal generation (Fig. 13). The field programmable gate array (FPGA) board with 2 channel ADC and digital-to-analog converter (DAC) (Sparatan3), generates the quadrature sinewave signal as the target doppler frequency.

The quadrature output signals from FPGA board (I/Q) are of low frequency and are converted into RF band by applying a single side band (SSB) modulator where the HMC521 chip is used.

The transmitted radar signal is received by receiver antenna, RX-ANT, and enters to the down converter and IF Amp. block where a HMC412 chips act as a mixer and a HMC778 chip for synthesizer1. The IF frequency output of down converter changes into digital signal by an ADC then goes to FPGA (Spartan-3). The DRFM techniques is applied for generation of target echo signal where delay and amplitude are selectable. The outputs of DRFM consist of inphase (I) and quadruture (Q) signals. The digital signals are first converted by DAC block, next analogs I

TABLE III
Relative Destruction Time Results With Different Values of $\frac{A_j}{A_s}$ and $\frac{B_j}{B_{R,\alpha}}$ for α = Velocity (Left Column) and α = Range (Right Column), $T_S = 2.5$ s, $\Delta f_j = 250$ MHz, $N = 25$, $S/J_{\text{(Velocity)}} = 6$ dB, and $S/J_{\text{(range)}} = 12$ dB

α=Velocity				α=Range			
$\frac{A_J}{A_S}(dB)$	$\frac{B_J}{B_{R,Velocity}}$	$T_{D,Velocity}(ms)$	$\frac{T_{D,Velocity}}{T_S}(\%)$	$\frac{A_J}{A_S}(dB)$	$\frac{B_J}{B_{R,Range}}$	$T_{D,Range}(ms)$	$\frac{T_{D,Range}}{T_S}(\%)$
-10	$\frac{10MHz}{150Hz}$	0	0	-20	$\frac{10MHz}{150Hz}$	0	0
-10	$\frac{1MHz}{150Hz}$	0	0	-20	$\frac{1MHz}{150Hz}$	0	0
-10	$\frac{100kHz}{150Hz}$	0	0	-20	$\frac{100kHz}{150Hz}$	0	0
-10	$\frac{10kHz}{150Hz}$	0	0	-20	$\frac{10kHz}{150Hz}$	0	0
-10	$\frac{1kHz}{150Hz}$	0	0	-20	$\frac{1kHz}{150Hz}$	0	0
0	$\frac{10MHz}{150Hz}$	100.0007	4.000028	-10	$\frac{10MHz}{150Hz}$	95.0017	3.800068
0	$\frac{1MHz}{150Hz}$	100.0075	4.0003	-10	$\frac{1MHz}{150Hz}$	95.017	3.80068
0	$\frac{100kHz}{150Hz}$	100.0746	4.002984	-10	$\frac{100kHz}{150Hz}$	95.17	3.8068
0	$\frac{10kHz}{150Hz}$	100.7464	4.029856	-10	$\frac{10kHz}{150Hz}$	96.7	3.868
0	$\frac{1kHz}{150Hz}$	107.4642	4.298568	-10	$\frac{1kHz}{150Hz}$	105.4	4.216
10	$\frac{10MHz}{150Hz}$	100.0014	4.000056	0	$\frac{10MHz}{150Hz}$	100.0013	4.000052
10	$\frac{1MHz}{150Hz}$	100.0142	4.000568	0	$\frac{1MHz}{150Hz}$	100.0131	4.000524
10	$\frac{100kHz}{150Hz}$	100.1425	4.0057	0	$\frac{100kHz}{150Hz}$	100.1311	4.005244
10	$\frac{10kHz}{150Hz}$	101.4246	4.056984	0	$\frac{10kHz}{150Hz}$	101.3107	4.052428
10	$\frac{1kHz}{150Hz}$	114.2464	4.569856	0	$\frac{1kHz}{150Hz}$	113.1071	4.524284
20	$\frac{10MHz}{150Hz}$	100.0015	4.00006	10	$\frac{10MHz}{150Hz}$	100.0015	4.00006
20	$\frac{1MHz}{150Hz}$	100.0149	4.000596	10	$\frac{1MHz}{150Hz}$	100.0148	4.000592
20	$\frac{100kHz}{150Hz}$	100.1492	4.005968	10	$\frac{100kHz}{150Hz}$	100.1481	4.005924
20	$\frac{10kHz}{150Hz}$	101.4925	4.0597	10	$\frac{10kHz}{150Hz}$	101.4811	4.059244
20	$\frac{1kHz}{150Hz}$	114.9246	4.596984	10	$\frac{1kHz}{150Hz}$	114.8107	4.592428
30	$\frac{10MHz}{150Hz}$	100.0015	4.00006	20	$\frac{10MHz}{150Hz}$	100.0015	4.00006
30	$\frac{1MHz}{150Hz}$	100.0150	4.0006	20	$\frac{1MHz}{150Hz}$	100.0150	4.0006
30	$\frac{100kHz}{150Hz}$	100.1499	4.005996	20	$\frac{100kHz}{150Hz}$	100.1498	4.005992
30	$\frac{10kHz}{150Hz}$	101.4992	4.059968	20	$\frac{10kHz}{150Hz}$	101.4981	4.059924
30	$\frac{1kHz}{150Hz}$	114.9925	4.5997	20	$\frac{1kHz}{150Hz}$	114.9811	4.599244
40	$\frac{10MHz}{150Hz}$	100.0015	4.00006	30	$\frac{10MHz}{150Hz}$	100.0015	4.00006
40	$\frac{1MHz}{150Hz}$	100.0150	4.0006	30	$\frac{1MHz}{150Hz}$	100.0150	4.0006
40	$\frac{100kHz}{150Hz}$	100.1500	4.006	30	$\frac{100kHz}{150Hz}$	100.1500	4.006
40	$\frac{10kHz}{150Hz}$	101.4999	4.059996	30	$\frac{10kHz}{150Hz}$	101.4998	4.059992
40	$\frac{1kHz}{150Hz}$	114.9992	4.599968	30	$\frac{1kHz}{150Hz}$	114.9981	4.599924
				40	$\frac{10MHz}{150Hz}$	100.0015	4.00006
				40	$\frac{1MHz}{150Hz}$	100.0150	4.0006
				40	$\frac{100kHz}{150Hz}$	100.1500	4.006
				40	$\frac{10kHz}{150Hz}$	101.5000	4.06
				40	$\frac{1kHz}{150Hz}$	114.9998	4.599992

and Q signals are converted into X-band by up converter block which uses HMC521 chip as the SSB modulator and HMC778 for synthesizer 2. The frequency difference between synthesizers 1 and 2 is equal to the desired doppler frequency (f_d).

The upconverter output after being amplified couples at TX-Ant and radiates in the other side. The jammer signal is generated by a jammer synthesizer which contains HMC778 chip. The center frequency and sweep band and its rate is selectable. The jammer synthesizer output after being amplified is reradiated through TX-Ant. Both the power of target and jammer signals are adjusted to obtain the specified j/s. For monitoring and adjusting the parameters, an excess down converter block is applied which contains simple synthesizer (MKU 10Bake/Cohne Electronic) as the local oscillator and HMC412 chip as the mixer. The jammer and the target test setup are illustrated in Fig. 14. In order to assess both the jammer and target echo signal spectrum

and to observe the jammer signal spectrum on the spectrum analyzer, a sample of the sending (or transmitted) signal is cached by the coupler. Both the input I and Q orthogonal signal spectrum enters to the SSB modulator and the output jammer signal spectrum are in this figure.

VII. EXPERIMENTAL RESULTS FOR OF THE ASSESSED JAMMER ON THE TRACKING RADAR BASED ON THE RELATIVE FUNCTIONALITY DESTRUCTION TIME CRITERION

The results obtained for relative functionality destruction time ($\frac{T_{D,\alpha}}{T_s}$) for different values of α, $\frac{A_j}{A_s}$, $\frac{B_j}{B_{R,\alpha}}$, and S/J, are tabulated in Tables II and III.

The approximation in this article consist of the following:

1) the jammer is of sweep barrage noise type;
2) the jammer power is much more than the thermal noise consequently, the thermal noise is neglected in the results extraction.

The relative functionality destruction time for different α parameters with varying $\frac{B_j}{B_R}$ depends on the amount of K_α^j and in the case $\alpha =$ range, the destruction rate starts at small value of j/s. At first, with the increase of j/s the destruction time will not increase much, but in the future, it will be greatly increased.

In this context, it is worth mentioning the following.

1) The Tables II and III are extracted when both the overhead (T_{OH}) and recovery (T_{renew}) times are not of concern.
2) If the expected destruction time is $T_{K,D,D} < 2$ s and by noting that $T_{K,D,\theta} < 8$ s to calculate the real receiver destruction time, $T_{\text{OH}} \simeq 100$ ms is added to the values of $T_{D,\alpha}$ in the Tables II and III, but the time $T_{\text{renew}} = 200$ ms is not added.
3) If the expected destruction time $T_{K,D,D} > 2$ s or $T_{K,D,\theta} > 8$s to calculate the real receiver destruction time for each one of the α parameter, the time $T_{\text{renew}} = 200$ ms is added to the results in the Tables II and III.

According to Tables II and III, it can be seen that in the very large $\frac{B_j}{B_R}$ cases (B_j=10 MHz, 1 MHz, and 100 kHz), with increasing of $\frac{A_j}{A_s}$ from -10 to 40 dB, destruction time increases (or proper functioning time decreases) and, depending on the value of $\frac{B_j}{B_R}$, remains almost constant, and the experimental results accommodates with the simulation results in Fig. 3. Also according to the experimental results through Tables II and III, it can be seen that for $\frac{A_j}{A_s}$ constant by increasing the $\frac{B_j}{B_R,\alpha}$ ratio, the relative destruction time ($\frac{T_{D,\alpha}}{T_s}$) reaches to a certain level which accommodates with the simulated curves in Fig. 6; moreover, as expected, if $\frac{A_j}{A_s}$ be too small (e.g., -10 dB), the receiver's performance will not be affected.

VIII. CONCLUSION

To evaluate the effect of jamming on tracking radar receiver, first, the relative functionality destruction time is introduced, where the power jammer signal to the target echo average ratio is of concern. The basis of this proposed method is on the analyses of the overlapping bands and the amount of energy injected in the receiver bandwidth from the jammer. The results of this criterion are obtained through modeling the sweep noise jamming effect on the radar receiver and calculating the relative functionality destruction time and the jamming effect coefficient. A search radar function together with noise jamming is assessed through Systemvue software, and the required STD of the noise for destruction of radar function is assessed. By using a real conical scan tracking radar, sweep noise jamming add together with a target with specific velocity and range, the expected results yield through proposed criteria for different conditions. Here, it is found that this newly proposed criterion outperforms its counterparts.

ACKNOWLEDGMENT

The authors here appreciate Isfahan University Radar Research Center (IURRC) for their complete assistance in providing their research facilities.

REFERENCES

[1] Z. Ying, Q. Gao, and Z. Wang
Modeling of jamming destroy factor
In *Proc. IEEE 4th Int. Congr. Image Signal Process.*, 2011, pp. 198–201.

[2] R. Klemm, W. Koch, and H. Griffiths
Novel Radar Techniques and Applications. London, U.K.: Institution of Engineering & Technology, 2017.

[3] Y. Zhu, Z. Wang, Q. Gao, and M. Jia
An effects evaluation method for angle deception jamming
In *Proc. IEEE 1st Int. Conf. Inf. Sci. Eng.*, 2009, pp. 4708–4711.

[4] J. Difranco and C. Kaiteris
Radar performance review in clear and jamming environments
IEEE Trans. Aerosp. Electron. Syst., vol. AES-17, no. 5, pp. 701–710, Sep. 1981.

[5] D. C. Schleher
Electronic Warfare in the Information Age. Norwood, MA, USA: Artech House, 1999.

[6] S. Neill
Electronic Warfare and Radar Systems Engineering Handbook. Sl: Military Bookshop, 2013.

[7] D. K. Barton
Radar System Analysis and Modeling, vol. 1. Norwood, MA, USA: Artech House, 2004.

[8] G. R. Curry
Radar System Performance Modeling, vol. 1. Norwood, MA, USA: Artech House, 2005.

[9] M. V. Maksimov *et al.*
Radar Anti-Jamming Techniques. Dedham, MA, USA: Artech House, 435 p. Translation., 1979.

[10] S. Paine, D. W. O'Hagan, M. Inggs, C. Schüpbach, and U. Böniger
Evaluating the performance of FM-based PCL radar in the presence of jamming
IEEE Trans. Aerosp. Electron. Syst., vol. 55, no. 2, pp. 631–643, Apr. 2019.

[11] E. K. Reedy
Radar ECCM considerations and techniques
In *Principles of Modern Radar*. Berlin, Germany: Springer, 1987, pp. 681–699.

[12] D. Feng, L. Xu, X. Pan, and X. Wang
Jamming wideband radar using interrupted-sampling repeater
IEEE Trans. Aerosp. Electron. Syst., vol. 53, no. 3, pp. 1341–1354, Jun. 2017.

[13] S. Mighani, M. Mivehchy, and M. F. Sabahi
Evaluating sweep noisy barrage jamming effect on tracking radar based on functioning destruction time
In *Proc. IEEE 7'th Int. Symp. Telecommun.*, 2014, pp. 400–404.

[14] C. Liu, R. Wu, Z. He, X. Zhao, H. Li, and P. Wang
Modeling and analyzing electromagnetic interference signal in complex battlefield environments
In *Proc. Int. Conf. Commun., Signal Process., Syst.*, 2016, pp. 351–361.

Mohammad Reza Zakerhaghighi received the B.Sc. degree in electrical engineering from the Shiraz University, Shiraz, Iran, and the M.Sc. degree in electrical engineering from the Kerman Graduate University of Technology, Kerman, Iran, in 2009 and 2013, respectively. He is currently working toward the Ph.D. degree electronic attack (EA) and electronic protection (EP) in radar system with Isfahan University, Isfahan, Iran.

From 2011, he was working on VHDL (hardware description language). His research interests include field programmable gate array, radio frequency building blocks for ultrawideband and millimeter-wave applications, distributed amplifier, and radar systems. His research focuses is on electronic countermeasure systems and electronic counter-countermeasure systems of radar systems.

Mohsen Mivehchy received the B.E. degree in electronic engineering and the M.E. degree in communication engineering from the Isfahan University of Technology, Isfahan, Iran, in 1987 and 1990, respectively, and the Ph.D. degree in electrical engineering from the University of Isfahan (UI), Isfahan, Iran, in 2010.

He is currently an Associate Professor with the Electrical Engineering Department, UI, where he has also been the Head of the RF and Microwave Circuits Research Center, since 2004. His current research interests include high-frequency circuits, system design, and radar systems.

Mohammad Farzan Sabahi (Member, IEEE) was born in Isfahan, Iran, in 1976. He received B.S. in electronics engineering, and M.S. degrees in communication engineering, and the Ph.D. degree in electrical engineering from the Isfahan University of Technology, Isfahan, Iran, in 1998, 2000, and 2008, respectively

From 2008, he has been a Faculty Member of Electrical Engineering Department, University of Isfahan, Isfahan, Iran. His main research interests include statistical signal processing, detection theory, and wireless communication.